

## Decorin blocks scarring and cystic cavitation in acute and induces scar dissolution in chronic spinal cord wounds



Zubair Ahmed <sup>\*1</sup>, Daljeet Bansal <sup>1</sup>, Katie Tizzard, Sarina Surey, Maryam Esmaili, Ana Maria Gonzalez, Martin Berry <sup>2</sup>, Ann Logan <sup>2</sup>

Neurotrauma and Neurodegeneration Section, School of Clinical and Experimental Medicine, University of Birmingham, Edgbaston, Birmingham B15 2TT, UK

### ARTICLE INFO

#### Article history:

Received 29 July 2013

Revised 30 November 2013

Accepted 12 December 2013

Available online 31 December 2013

#### Keywords:

Spinal cord injury

Decorin

ECM

Scarring

MMP

TIMP

tPA

### ABSTRACT

In the injured central nervous system (CNS), transforming growth factor (TGF)- $\beta$ 1/2-induced scarring and wound cavitation impede axon regeneration implying that a combination of both scar suppression and axogenic treatments is required to achieve functional recovery. After treating acute and chronic dorsal funicular spinal cord lesions (DFL) in adult rats with the pan-TGF- $\beta$ 1/2 antagonist Decorin, we report that in: (1), acute DFL, the development of all injury parameters was significantly retarded e.g., wound cavity area by 68%, encapsulation of the wound by a glia limitans accessoria (GLA) by 65%, GLA basal lamina thickness by 94%, fibronectin, NG2 and Sema-3A deposition by 87%, 48% and 48%, respectively, and both macrophage and reactive microglia accumulations by 60%; and (2), chronic DFL, all the above parameters were attenuated to a lesser extent e.g., wound cavity area by 11%, GLA encapsulation by 25%, GLA basal lamina thickness by 31%, extracellular fibronectin, NG2 and Sema-3A deposition by 58%, 22% and 29%, respectively, and macrophage and reactive microglia accumulations by 44%. Moreover, in acute and chronic DFL, levels of tissue plasminogen activator (tPA) were raised (by 236% and 482%, respectively), as were active-MMP-2 (by 64% and 91%, respectively) and active-MMP-9 (by 122% and 18%, respectively), while plasminogen activator inhibitor-1 (PAI-1) was suppressed (by 56% and 23%, respectively) and active-TIMP-1 and active-TIMP-2 were both lower but only significantly suppressed in acute DFL (by 56 and 21%, respectively). These findings demonstrate that both scar tissue mass and cavitation are attenuated in acute and chronic spinal cord wounds by Decorin treatment and suggest that the dominant effect of Decorin during acute scarring is anti-fibrogenic through suppression of inflammatory fibrosis by neutralisation of TGF- $\beta$ 1/2 whereas, in chronic lesions, Decorin-induction of tPA and MMP (concomitant with reduced complementary levels of TIMP and PAI-1) leads to dissolution of the mature established scar by fibrolysis. Decorin also promoted the regeneration of similar numbers of axons through acute and chronic wounds. Accordingly, intrathecal delivery of Decorin offers a potential translatable treatment for scar tissue attenuation in patients with spinal cord injury.

© 2014 Elsevier Inc. All rights reserved.

### Introduction

The realisation that spinal cord axon regeneration is limited after injury by potent scar-derived axon growth inhibitory ligands has driven the search for clinically effective anti-scarring agents which enhance pro-regenerative treatment strategies (Kawano et al., 2012). While a number of studies have reported modulation of wound cavitation and acute fibrotic scar development in the injured CNS (Logan et al.,

1999a, 1999b, 1994; Davies et al., 2004, 2006; Minor et al., 2008), pharmacological manipulation of mature scars has not been attempted and strategies to reduce cavitation have not been developed.

Three distinct sequential phases in the cellular responses of the adult rat CNS to penetrant injury (Berry et al., 1983; Lagord et al., 2002) are recognised: (1), an *acute haemorrhagic phase*, when haematogenous inflammatory cells invade the lesion, and when the severed proximal stumps of axons begin to sprout; (2), a *sub-acute phase* when scarring commences as reactive astrocytes interact with invading meningeal fibroblasts to produce a glia limitans about the wound cavity (glia limitans accessoria – GLA) with a core of ECM proteins, revascularisation gets underway and axon growth is arrested at the wound margins (abortive axon regeneration); and (3), a *consolidation phase* when the ECM deposits are remodelled by proteases to establish the mature contracted scar. In the spinal cord, the superimposition of progressive wound cavitation on the above programme culminates in the progressive cystic expansion of an astrocyte-free void within the wound filled

\* Corresponding author at: Neurotrauma and Neurodegeneration Section, School of Clinical and Experimental Medicine, College of Medical and Dental Sciences, Institute of Biomedical Research (West), University of Birmingham, Edgbaston, Birmingham B15 2TT, UK. Fax: +44 121 414 8867.

E-mail address: [zahmed.1@bham.ac.uk](mailto:zahmed.1@bham.ac.uk) (Z. Ahmed).

Available online on ScienceDirect ([www.sciencedirect.com](http://www.sciencedirect.com)).

<sup>1</sup> These authors contributed equally to this work.

<sup>2</sup> Joint senior authors.

with proteoglycans and macrophages and bordered by a proteoglycan-rich neuropil that causes secondary destruction of axons (Butt et al., 2002; Fitch et al., 1999; Lagord et al., 2002; Pasterkamp et al., 1999, 2001; Tang et al., 2003). Moreover, the failure of CNS axons to regenerate after injury is attributed to a plethora of axon growth inhibitory ligands, including chondroitin sulphate proteoglycans (CSPG), semaphorins (Sema) and ephrins, that accumulate in and around the developing lesion (Sandvig et al., 1994).

After disruption of the blood–brain barrier in the acute phase, injury responsive cells release multiple cytokines, principal amongst which are the transforming growth factors- $\beta$ 1/2 (TGF- $\beta$ 1/2) initially released from extravasated platelets and later from macrophages and reactive glia (Logan et al., 1994). Binding of TGF- $\beta$ 1/2 to the TGF- $\beta$  receptor initiates Smad intracellular signalling and downstream transcriptional and post-translational regulation of multiple genes and their products (Xu et al., 2012). Platelet-derived TGF- $\beta$ 1/2 stimulate astrogliosis and chemo-attract haematogenous TGF- $\beta$ 1/2-secreting ED1<sup>+</sup> macrophages into the wound, which initiate fibrotic scarring and neovascularisation (Boche et al., 2006; Lagord et al., 2002, 1999b; Silver and Miller, 2004), clear necrotic debris and suppress plasminogen activator inhibitor-1 (PAI-1) (Minor et al., 2008; Samarakoon et al., 2013; Yang et al., 2011) that disinhibits tissue plasminogen activator (tPA), thereby contributing to the development of wound cavities (Fitch et al., 1999; Lagord et al., 2002; Zhang et al., 1997) and scar remodelling. TGF- $\beta$ 1/2 mRNA levels rapidly rise in the cord during the acute phase of wounding, although peak titres of TGF- $\beta$ 2 mRNA are lower than those of TGF- $\beta$ 1 (Lagord et al., 2002). Administration of exogenous TGF- $\beta$ 1 increases ECM deposition in CNS lesions (Logan et al., 1994; Zhang et al., 1997), while antibodies to TGF- $\beta$ 1/2 suppress CNS scarring and inflammation (Logan et al., 1994). A similar reduction of CNS scarring is achieved with LY-364947, a small molecule inhibitor of the TGF- $\beta$  receptor (Yoshioka et al., 2011).

Decorin is a naturally occurring extracellular small leucine-rich proteoglycan TGF- $\beta$ 1/2 antagonist, which regulates diverse cellular functions through interactions with components of the ECM (Davies et al., 2004; Hocking et al., 1998; Logan et al., 1999a). Decorin suppresses CNS scarring by: (1), attenuating both TGF- $\beta$ 1/2 receptor activation and signalling through down-stream Smads that mediate transcriptional activation of ECM production (Akhurst, 2006; Yamaguchi et al., 1990); (2), binding to type I collagen fibrils to inhibit fibrogenesis (Reese et al., 2013); (3), forming an activity-blocking complex with connective tissue growth factor (CTGF) (Vial et al., 2011); (4), binding to fibronectin and inhibiting cell adhesion and fibroblast migration (Winnemoller et al., 1991); (5), abrogating inflammation, CSPG/laminin/fibronectin-rich scar formation (Davies et al., 2004) and the

injury responses of astrocytes, microglia and macrophages (Davies et al., 2004, 2006; Lagord et al., 2002, 1999a); (6), stimulating microglia to secrete plasminogen/plasmin (the activity of which is moderated by PAI-1; Renckens et al., 2005), which then regulates matrix metalloproteinase (MMP):tissue inhibitors of MMP (TIMP) ratios in wounds to initiate fibrolytic degradation of ECM underpinning remodelling during the consolidation phase of acute scarring (Davies et al., 2006); and (7) binding to the epidermal growth factor receptor (EGFR), hepatocyte growth factor (Met) receptor and toll-like receptors to modulate angiogenesis (Neill et al., 2012) and inflammatory responses (Hamada et al., 1996). Decorin also promotes axon regeneration either directly by suppressing the production of scar-derived growth inhibitory ligands or indirectly by: (1), plasmin activation of neurotrophins (Davies et al., 2006); (2), disinhibition of axon growth cone advance by digestion of CSPG and CNS myelin inhibitors through plasmin and plasmin-induced activation of MMP (Minor et al., 2008); and (3), suppression of EGFR activity in growth cones, thereby blocking CSPG/CNS myelin mediated growth cone collapse, although Douglas et al. (2009) and Berry et al. (2011) claim that activation of EGFR does not trigger the inhibitory signalling cascade.

We hypothesise that Decorin treatment, commenced immediately after spinal cord injury, inhibits TGF- $\beta$ 1/2-mediated invasion of inflammatory cells, scar deposition and cavitation and that later, during the consolidation phase, regulates ECM remodelling by both the induction of MMP and tPA activity and suppression of TIMP and PAI-1. Moreover, in Decorin-treated mature scars in which acute titres of TGF- $\beta$ 1/2 have declined, we suggest that scar dissolution is induced by MMP/tPA-mediated fibrolytic activities and enhanced by depressed levels of TIMP and PAI-1 activity. This study tests the above hypotheses, predicting that Decorin suppresses acute scarring (fibrogenesis) and wound cavitation, and induces dissolution of mature scar tissue (fibrolysis) in dorsal funicular lesions (DFL) of the spinal cord of the adult rat.

## Materials and methods

### Surgical procedures and design of experiments

All surgical procedures and experimental protocols were licensed by the UK Home Office and approved by the University of Birmingham Ethical Review Sub-Committee. Adult male Sprague Dawley rats (200–250 g) were kept in environmentally controlled animal facilities at the University of Birmingham. DFL were positioned at the level of T8 penetrating to a depth of 1.5 mm, as described by us previously (Lagord et al., 2002) under inhalation anaesthesia using 5% isoflurane

**Table 1**  
List of primary antibodies used.

Antibody	Specificity	Dilution	Source
<i>Mouse</i>			
CSPG (CS56)	Chondroitin sulphate proteoglycan	1:200	Sigma, Poole, UK
ED1	Macrophages	1:200	Serotec, Kidlington, UK
GFAP	Astrocytes	1:400	Sigma, Poole, UK
GAP43	Regenerating axons	1:500	Invitrogen, Paisley, UK
<i>Rabbit</i>			
Fibronectin	ECM protein	1:200	Sigma, Poole, UK
Laminin (Lam)	Basal lamina/glia limitans and blood vessels	1:200	Sigma, Poole, UK
NG2	NG2-expressing synantocytes	1:400	Millipore, Watford, UK
Raldh-2	Meningeal fibroblasts	1:1000	P.J. McCaffery, University of Aberdeen, UK
Sema-3A	Semaphorin 3A	1:200	Abcam, Cambridge, UK
MMP-2	Matrix metalloproteinase-2	1:200	Santa Cruz, CA, USA
MMP-9	Matrix metalloproteinase-9	1:200	Santa Cruz, CA, USA
TIMP-1	Tissue inhibitor of metalloproteinases-1	1:200	Santa Cruz, CA, USA
TIMP-2	Tissue inhibitor of metalloproteinases-2	1:200	Santa Cruz, CA, USA
tPA	Tissue plasminogen activator	1:200	Santa Cruz, CA, USA
PAI-1	Plasminogen activator inhibitor-1	1:1000	Abcam, Cambridge, UK

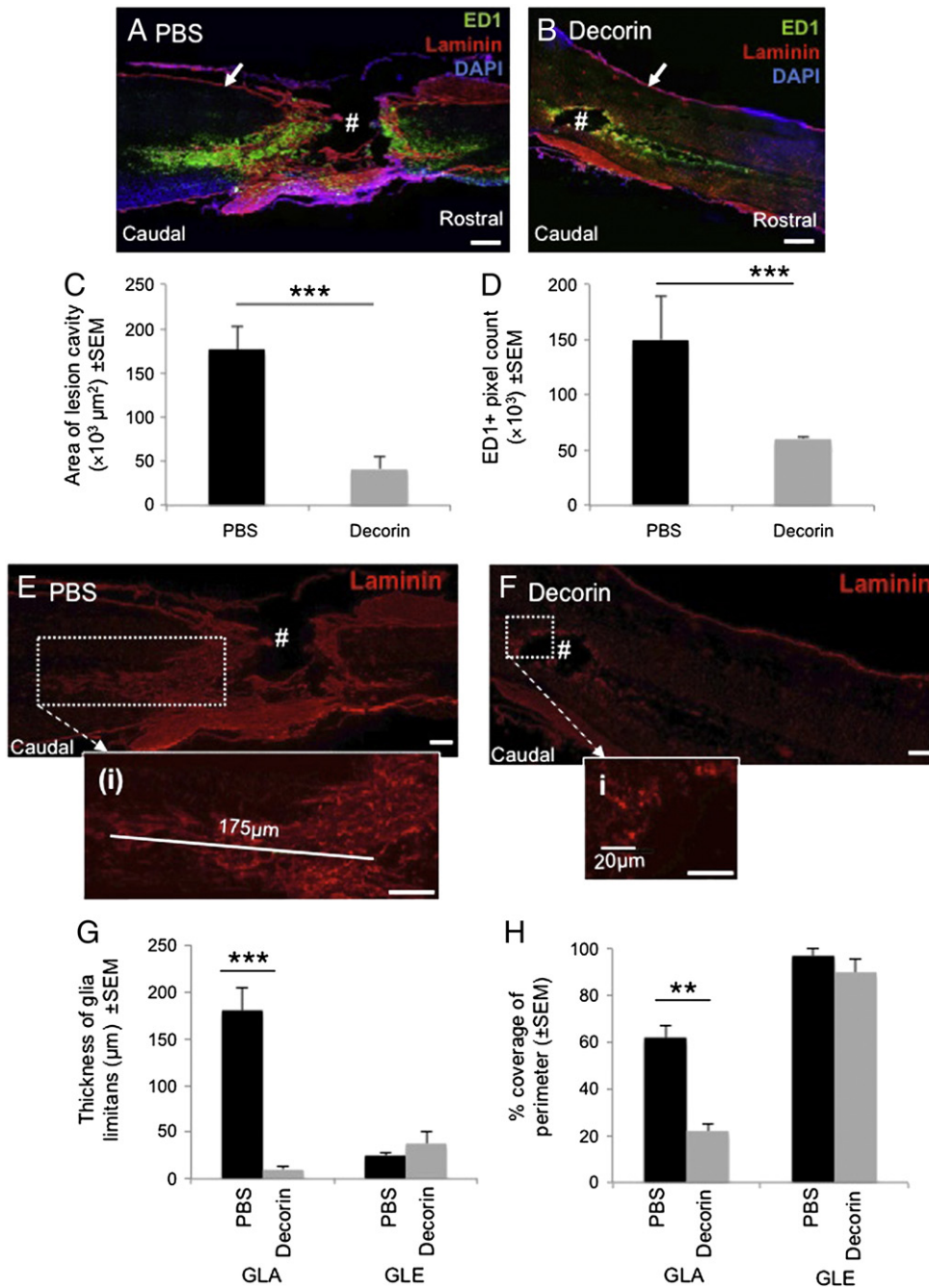


**Fig. 1.** Decorin suppresses macrophage invasion, the formation of a GLA and wound cavitation in acute DFL (ED1, laminin and DAPI immunostaining). (A) Representative PBS-treated lesion with an area of  $0.69 \text{ mm}^2$ . (B) Representative Decorin-treated wound cavity with an area of  $0.31 \text{ mm}^2$ . The laminin staining defines the GLA and GLE (arrows), and ED1 identifies haematogenous macrophages. (C) ED1<sup>+</sup> quantification of PBS- and Decorin-treated lesions (ED1 pixel count). Laminin immunostaining to measure formation of the GLA: (E) after PBS and (F) Decorin treatments. Insets (E(i)) and (F(i)) show details of respective areas and thickness of the GLA at higher magnifications; # = lesion epicentre. (G) Quantification of laminin staining to show coverage of lesion perimeter and (H) thickness of the laminin<sup>+</sup> basal lamina of the GLA in DFL, and the GLE (\*\* $p < 0.01$ ; \*\*\* $p < 0.001$ ;  $n = 6$ ; # = lesion epicentre, scale bars =  $100 \mu\text{m}$ ).

(IsoFlo, Abbott Animal Health, North Chicago, IL, USA) for induction and 2% for maintenance.

#### Experiment 1 – effects of Decorin on acute DFL

The dorsal funiculi of 12 rats were lesioned on day 0, when freeze-dried collagen matrices were immediately implanted into DFL sites and injected with  $2 \mu\text{l}$  of recombinant human Decorin (Galacarin, Catalent Pharma Solutions, Middleton, UK), at a concentration of  $4.87 \mu\text{g}/\mu\text{l}$ , using glass micropipettes. The peri-lesion neuropil 5 mm rostral and caudal to DFL was also injected with  $2 \mu\text{l}$  recombinant

human Decorin ( $4.87 \mu\text{g}/\mu\text{l}$ , Supplementary Fig. 1A). Rats were killed 21 days post lesion (dpl) and intracardially perfused with 4% paraformaldehyde (TAAB Labs, Berkshire, UK). Segments of the cord containing the lesion site were post-fixed in 4% paraformaldehyde for 2 h, cryoprotected in a graded series of sucrose, embedded in OCT (R.A. Lamb, East Sussex, UK) and stored at  $-80^\circ\text{C}$  until required.

#### Experiment 2 – effects of Decorin on chronic DFL

The dorsal funiculi of 6 rats were lesioned on day 0 and the scar allowed to mature over the next 21 days when cords were re-exposed

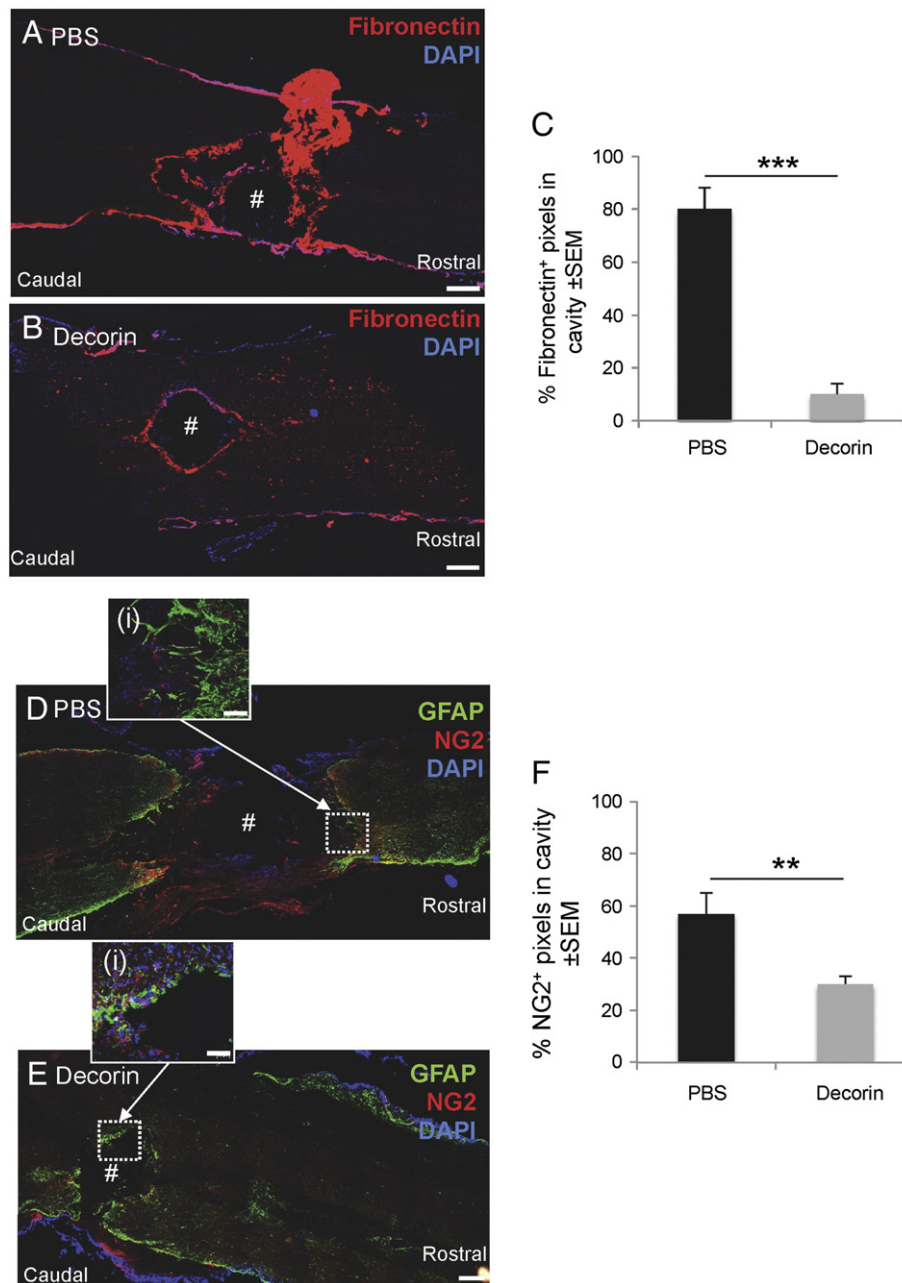


**Fig. 2.** Decorin suppresses fibronectin and NG2 deposition of acute DFL. Immunostaining of fibronectin after: (A) PBS and (B) Decorin treatments. (C) Quantification of areas of wound cavity containing fibronectin in PBS- and Decorin-treated lesions. Double immunostaining of GFAP<sup>+</sup> reactive astrocytes and NG2<sup>+</sup> synantocytes after: (D) PBS and (E) Decorin treatments; (i) inserts show the magnified area in the boxed panels. (F) Quantification of NG2<sup>+</sup> immunostaining in lesion cavity in PBS- and Decorin-treated lesions (nuclei are DAPI-stained; \**p* < 0.05; \*\*\**p* < 0.001; *n* = 6; # = lesion epicentre, scale bars = 100 μm).

and freeze-dried collagen matrices placed on the pia mater over the lesion and injected with 2 μl of recombinant human Decorin (4.87 μg/μl). DFL and peri-lesion neuropil 5 mm rostral and caudal to the DFL were also injected with 2 μl recombinant human Decorin (4.87 μg/μl, Supplementary Fig. 1B). Rats were killed 14 days later, intracardially perfused with 4% paraformaldehyde and spinal cords embedded in OCT and stored as described in *Experiment 1*.

#### Control groups

Lesion treatment protocols and animal numbers for control groups were identical to those described for *Experiments 1 and 2*, but PBS was substituted for Decorin for all injections into collagen matrices, DFL and peri-DFL neuropil.

#### Preparation of collagen matrix implants

Bovine collagen I (Cell Prime, Cohesion Technologies Inc., Palo Alto, CA, USA) was neutralised with 1 M sodium phosphate and aliquots of 20 μl were freeze-dried overnight in Eppendorf tubes to form individual matrix pellets that were stored at –80 °C until implantation into DFL sites.

#### Immunohistochemistry

OCT embedded spinal cords were sectioned longitudinally using a cryostat (Bright Instruments, Huntingdon, UK) and adhered onto Xtra™ adhesive slides (Surgipath, Peterborough, UK) and immunohistochemistry performed as described previously (Ahmed et al., 2005).

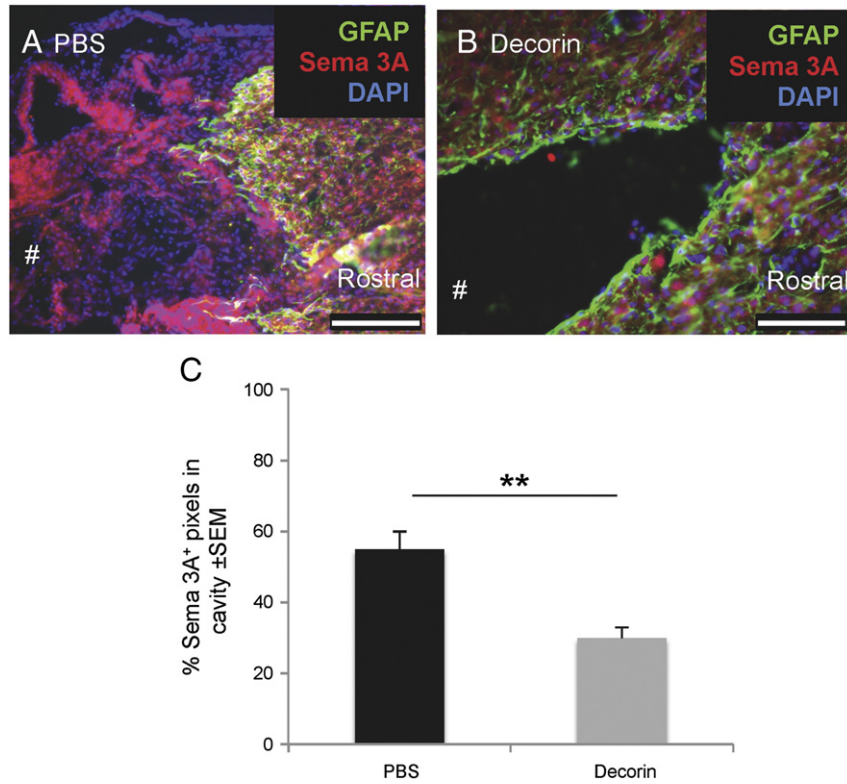


**Fig. 3.** Decorin suppresses Sema-3A in acute DFL. Immunostaining rostral to the lesion of GFAP and Sema-3A after: (A) PBS and (B) — Decorin treatments. (C) Quantification of the area occupied by Sema-3A immunostaining in PBS- and Decorin-treated lesions (\*\* $p < 0.01$ ;  $n = 6$ ; # = lesion epicentre, scale bars = 100  $\mu\text{m}$ ).

Briefly, sections were washed 3 $\times$  in PBS, and blocked for 1 h at room temperature (RT) in PBS containing 3% (w/v) BSA and 0.1% (v/v) Triton X-100. Sections were immersed in primary antibodies (detailed in Table 1) prepared in blocking buffer, incubated overnight at 4  $^{\circ}\text{C}$ , washed 3 $\times$  in PBS and incubated with appropriate Alexa Fluor 488 (green) and Texas Red (red) anti-mouse and anti-rabbit IgG secondary antibodies, prepared in blocking buffer for 1 h at RT. Negative staining was recorded in all specific secondary antibody binding controls included in each run, in which the primary antibody was omitted. All sections were mounted on slides with Vectashield<sup>TM</sup> for fluorescence with DAPI (Vector Laboratories Inc., Peterborough, UK) and examined using a fluorescent microscope (Carl Zeiss, Hertfordshire, UK) equipped with an AxioCam HRc (Carl Zeiss). Images were captured using the Axiovision Software (Carl Zeiss).

#### Image analysis and quantification of immunostaining

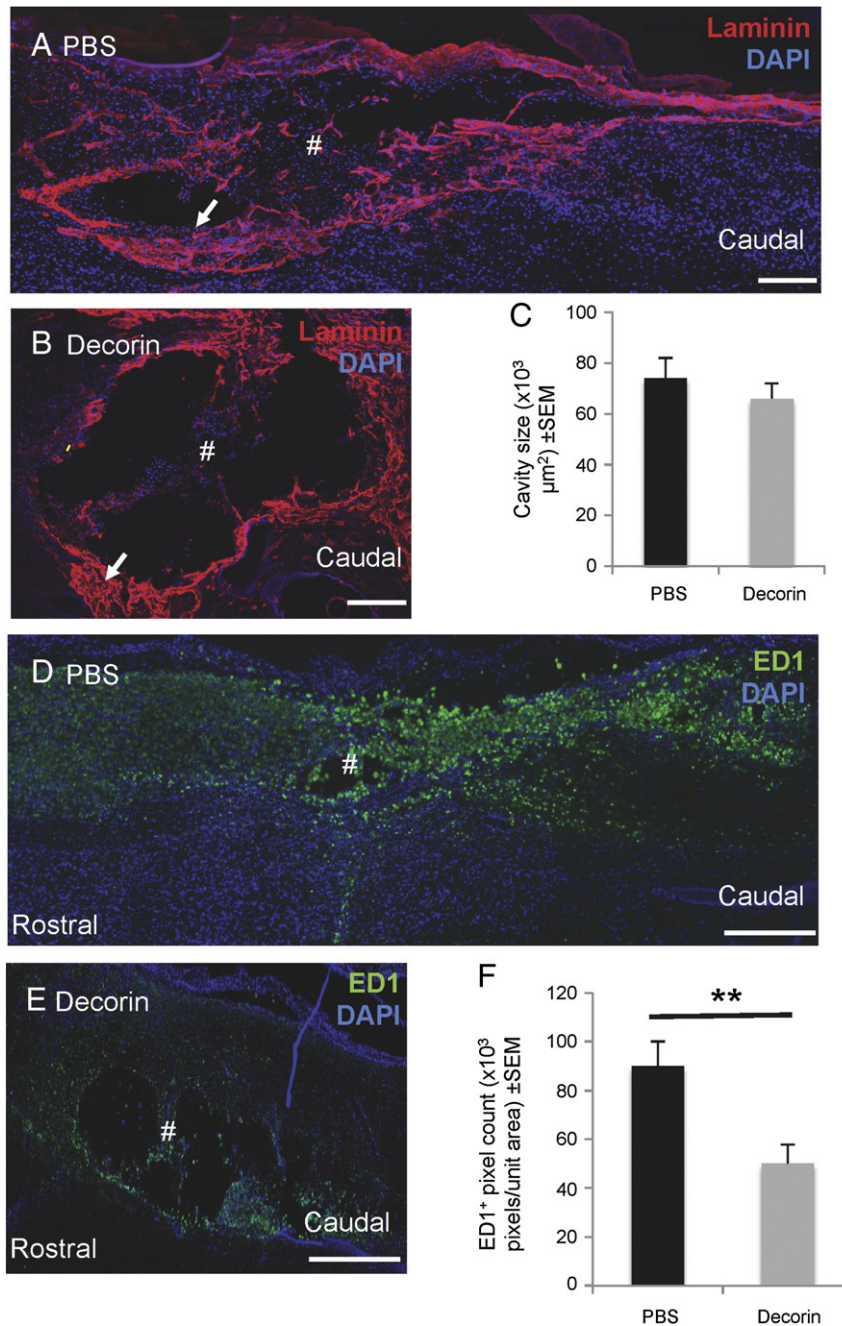
To eliminate sample bias caused by the variation in size of the wound cavity in sections at different wound depths, cavity sizes in sections taken from similar depths in each animal were compared and quantified (e.g. Supplementary Fig. 2). For each protein, 3 sections from defined depths through the cord from 6 different animals from each treatment groups was analysed.

Image-Pro Analyzer 6.2 (Media Cybernetics Inc. Bethesda, MD, USA) was used for quantification of all immunostaining after setting the background threshold levels using antibody control sections (omission of primary antibody). The lesion perimeter was outlined to delimit the total area of the cavity and % coverage of the total lesion perimeter by the GLA estimated in 5 random quadrants around the cavity perimeter (Supplementary Fig. 1C – GLA). The thickness of the basal lamina of the GLA in 5 random quadrants about the wound cavity perimeter was normalised as % thickness of the basal lamina of the unaffected intact glia limitans externa (GLE), the thickness of which was unchanged

by Decorin treatment. The numbers of pixels with a fluorescence intensity above the background threshold for ED1 were counted in 5 random quadrants in the neuropil around the wound cavity (one side of the quadrant was an arc on the cavity perimeter (Supplementary Fig. 1C – ED1) and expressed as pixel number/unit area). The numbers of pixels with an intensity of fibronectin, NG2 and Sema-3A fluorescence above background threshold in the wound cavity were counted and expressed as % total pixel number in the measured sector.

#### Tissue lysis and western blotting for MMP, TIMP, tPA and PAI-1

Tissues extending 3 mm on either side of the DFL epicentre ( $n = 6$  rats/treatment group) were removed and divided into 3 sample sets, containing the pooled tissue from 2 animals from which total protein was extracted by homogenisation in ice-cold lysis buffer containing 20 mM Tris HCl, 1% NP-40, 3 mM EDTA and 3 mM EGTA (Ahmed et al., 2005). Briefly, tissue lysates were clarified by centrifugation at 13,000  $\times g$  for 20 min at 4  $^{\circ}\text{C}$ , protein content assayed by a Biorad DC protein assay and 40  $\mu\text{g}$  of total protein run on 12% SDS-PAGE gels. Proteins were then transferred onto PVDF membranes (Sigma, Poole, UK) and probed with relevant antibodies (Table 1) overnight at 4  $^{\circ}\text{C}$  with constant agitation. Membranes were then washed 3 $\times$  in Tris-buffered saline containing 0.05% Tween-20 (Sigma) (TTBS) and incubated with the appropriate HRP-labelled secondary antibody (GE Healthcare, Buckinghamshire, UK) followed by 3 $\times$  washes in TTBS. Reactive bands were visualised using an enhanced chemiluminescent system (ECL) (GE Healthcare), scanned using Adobe Photoshop and densitometrically analysed using the built-in gel plotting macros in ImageJ (NIH, USA). Each blot was run on 3 independent occasions and the amount of enzyme present in each band of interest expressed as mean integrated density  $\pm$ SEM. MMP:TIMP and tPA:PAI-1 ratios were also calculated from mean integrated density values.



**Fig. 4.** Cavity size and macrophage invasion in treated DFL wounds. Immunostaining of laminin defines the perimeter of GLA (arrows) in: (A) PBS- and (B) Decorin-treated DFL. (C) Quantification of the lesion site in PBS- and Decorin-treated DFL. ED1<sup>+</sup> macrophage invasion in chronic DFL after: (D) PBS- and (E) Decorin treatments. (F) Quantification of ED1 pixel counts for PBS- and Decorin-treated chronic DFL (nuclei are DAPI-stained; # = lesion epicentre; n = 6, scale bars = 100  $\mu\text{m}$ ).

### Zymography

Zymography was used to analyse gelatinase activity in DFL in PBS control and Decorin-treated animals, based on our previously published methods (Ahmed et al., 2005). Briefly, the spinal cord extending 3 mm on either side of the DFL epicentre was isolated from 6 rats/treatment group and divided into 3 sample sets each containing the pooled tissue from 2 animals. Each sample set was homogenised without the inclusion of protease inhibitors and 40  $\mu\text{g}$  of total protein resolved on commercially available 10% minigels incorporated with gelatin substrate (Invitrogen, Paisley, UK). Minigels were washed in renaturing buffer (Invitrogen) and incubated overnight at 37 °C in developing buffer (Invitrogen). After staining the minigels in 0.5% Coomassie Blue, clear

protein lysis bands on a blue background were visualised and scanned using Adobe Photoshop software (San Jose, CA, USA). Densitometric analysis of digested bands of interest from 3 separate zymograms was performed by measuring the integrated density of the bands using the built-in gel plotting macros in ImageJ (NIH), as described above.

### Statistical analysis

Sample means and SEM were calculated and statistical significances assessed with SPSS statistical analysis software version 15.0 (SPSS Inc., Chicago, Illinois, USA), using an independent t-test to compare Decorin versus PBS treated groups.

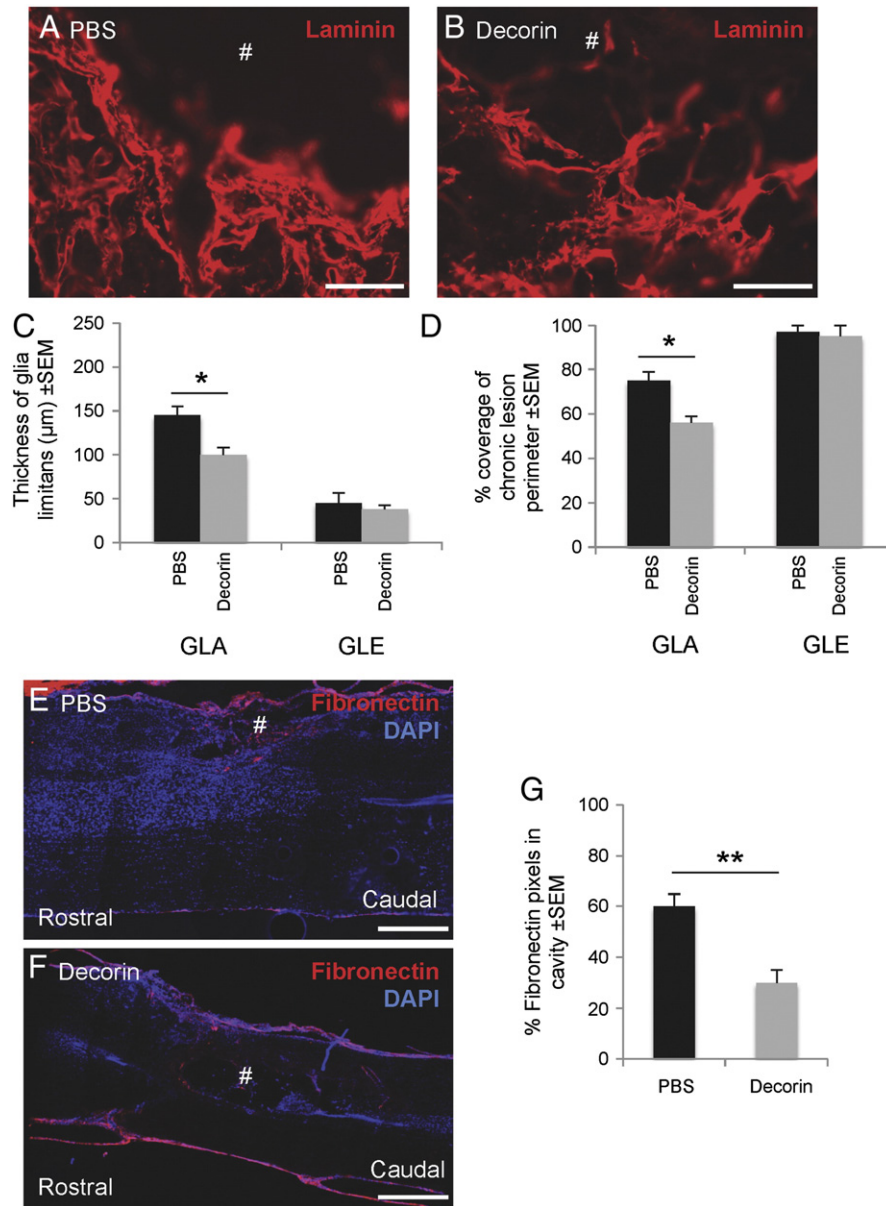


**Fig. 5.** Assessment of GLA and GLE and reduction of fibronectin levels after Decorin treatment in chronic DFL. Laminin<sup>+</sup> basal lamina of the GLA after (A) PBS- and (B) Decorin-treatments. Thickness of the GLA and % coverage of chronic DFL by GLA after: (C) PBS and (D) Decorin treatments. Decorin also reduced fibronectin levels in chronic DFL after: (E) PBS and (F) Decorin treatments. (G) Quantification of fibronectin levels after PBS and Decorin treatments (nuclei are DAPI-stained; # = lesion epicentre; \*p < 0.05; \*\*p < 0.001; n = 6; scale bars = 100 µm).

## Results

### Effect of Decorin on acute DFL inflammatory scar formation

Decorin treatment suppressed DFL cavity area by 77% (Figs. 1A–C) ( $40 \times 10^3 \mu\text{m}^2 \pm 1.4 \times 10^3$  in Decorin-treated compared to  $176 \times 10^3 \mu\text{m}^2 \pm 2.5 \times 10^3$  in PBS controls –  $p < 0.0001$ ), an effect that was independent of lesion depth (Supplementary Fig. 2). ED1<sup>+</sup> macrophage infiltration into DFL neuropil was suppressed by 60% ( $60 \times 10^3 \pm 2.1 \times 10^3$  ED1<sup>+</sup> pixels/unit area in Decorin-treated compared with  $150 \times 10^3 \pm 40 \times 10^3$  ED1<sup>+</sup> pixels/unit area in PBS controls –  $p < 0.0001$ ) (Figs. 1A, B and D). The basal lamina of the GLA was defined by a thick multi-laminated laminin-rich membrane in PBS-treated controls compared to Decorin-treated lesions in which the lesion boundary was poorly defined, fragmented and thinned by 94% ( $10 \pm 3 \mu\text{m}$  in Decorin-treated compared to  $180 \pm 7 \mu\text{m}$  in PBS controls – Figs. 1E–G) and encapsulated only  $20 \pm 3.4\%$  of the DFL cavity perimeter after

Decorin treatment compared with  $62 \pm 2.1\%$  in PBS-treated controls, a reduction of 68% ( $P < 0.0001$ ) (Fig. 1H). The thickness and continuity of the GLE of the pia mater was unaffected by Decorin treatment (Figs. 1E–H).

All scar-related ECM elements measured were present at significantly lower levels in the Decorin-treated compared to PBS control DFL, for example: (1), the area of fibronectin deposition in the wound cavity was reduced by 87% (10% in Decorin-treated rats compared to 78% in PBS controls –  $P < 0.0001$ ) (Figs. 2A–C); (2), the area of proteoglycan NG2 immunostaining in the wound cavity was reduced by 48% (30% in Decorin-treated rats compared to 58% in PBS controls –  $P < 0.05$ ) (Figs. 2D, D(i), E, E(i) and F); (3), Sema-3A immunostaining in the wound cavity (Figs. 3A and B) was reduced by 48% (30% in Decorin-treated rats compared to 58% in PBS controls –  $P < 0.05$ ) (Fig. 3C).

In both PBS control (Figs. 2D and 3A) and Decorin-treated (Figs. 2E and 3B) groups, GFAP staining was widespread in the neuropil around the lesion cavity, with evidence of some astrocyte migration into the

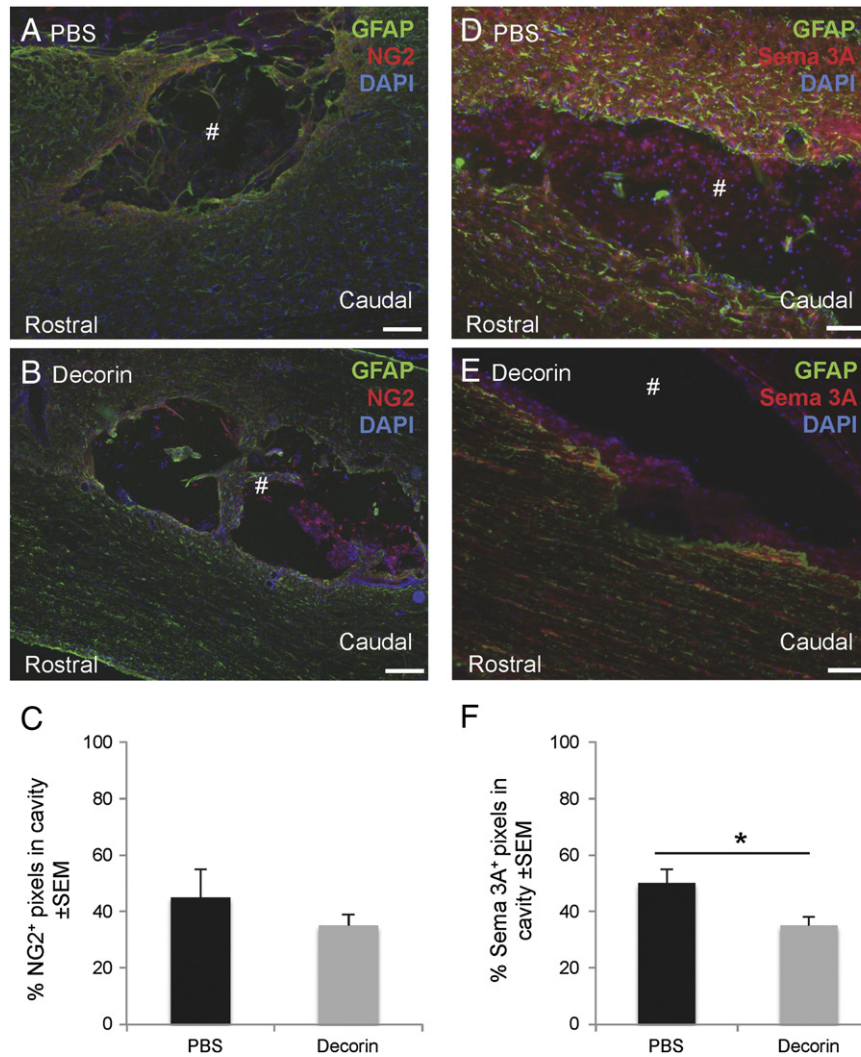


**Fig. 6.** Decorin reduces NG2 and Sema-3A levels within chronic DFL wound cavities. Immunostaining of NG2 after: (A) PBS and (B) Decorin treatments and (C) quantification of the area of NG2 staining in PBS- and Decorin-treated DFL. Sema-3A levels in chronic DFL cavities after: (D) PBS and (E) Decorin treatments. (F) Quantification of the area of Sema-3A staining in PBS- and Decorin-treated DFL (nuclei are DAPI-stained; n = 6; # = lesion epicentre; \*p < 0.05; scale bars = 100  $\mu$ m).

cavity in PBS-treated groups (Figs. 2D(i)). Astrocyte processes juxtaposed to the GLA were also thicker, more elongated and aligned along the GLA after PBS (Figs. 2D(ii)) than after Decorin treatment (Figs. 2E(i)). In Decorin- and PBS-treated rats, GFAP<sup>+</sup> reactive astrocyte processes lined the lesion cavity but were not present within the lesion cavity (Figs. 3A and B).

These results demonstrate that the commencement of Decorin treatment immediately after trauma suppressed inflammation, scar deposition and wound cavitation in acute DFL.

#### Effect of Decorin on chronic DFL scar dissolution

The relative stability of ECM parameters in the DFL of PBS-treated rats between the acute (21 dpi) and chronic (35 dpi) studies indicated that by 21 days the scar was mature validating our chronic spinal cord injury model. However, in chronic DFL, surgical re-exposure of the injury site and subsequent coverage with matrix, and perilesion injections was invasive and associated with inflammation, as evidenced by the fresh accumulation of ED1<sup>+</sup> macrophages and reactive microglia about the wound.

Decorin treatment reduced all measured parameters of the mature DFL scar including: (1), cavity area by 11% ( $66 \times 10^3 \mu\text{m}^2 \pm$

$8 \times 10^3$  in Decorin-treated rats compared to  $74 \times 10^3 \mu\text{m}^2 \pm 6 \times 10^3$  in PBS controls; not significant) (Figs. 4A–C), an effect that was independent of lesion depth (not shown); (2), ED1<sup>+</sup> cell accumulation by 44% ( $50 \times 10^3 \pm 8 \times 10^3$  pixels/unit area in PBS controls compared to  $90 \times 10^3 \pm 10 \times 10^3$  pixels/unit area in Decorin treated rats – p < 0.001) (Figs. 4D–F); (3), basal lamina thickness of the GLA by 31% ( $100 \pm 10 \mu\text{m}$  in Decorin-treated rats compared to  $145 \pm 12 \mu\text{m}$  in PBS controls – p < 0.01); and (4) GLA basal lamina coverage of the wound cavity perimeter by 25% (56% in Decorin-treated rats versus 75% in PBS-treated rats – P < 0.01) (Figs. 5A–D). The GLE was unaffected by Decorin (Figs. 5C and D).

All scar-related ECM elements measured were present at lower levels in Decorin- compared to PBS-treated chronic DFL, for example: (1), the area of fibronectin deposition within the cavity was 58% lower (25% in Decorin-treated rats compared to 60% in PBS controls – P < 0.001) (Figs. 5E–G); (2), the area of NG2 staining within the cavity was 22% lower (35% in Decorin-treated rats compared to 45% in PBS controls; not significant; Figs. 6A–C); (3), the area of Sema-3A immunostaining within the cavity was 29% lower (39% in Decorin-treated rats compared to 55% in PBS controls – P < 0.05, Figs. 6D–F).

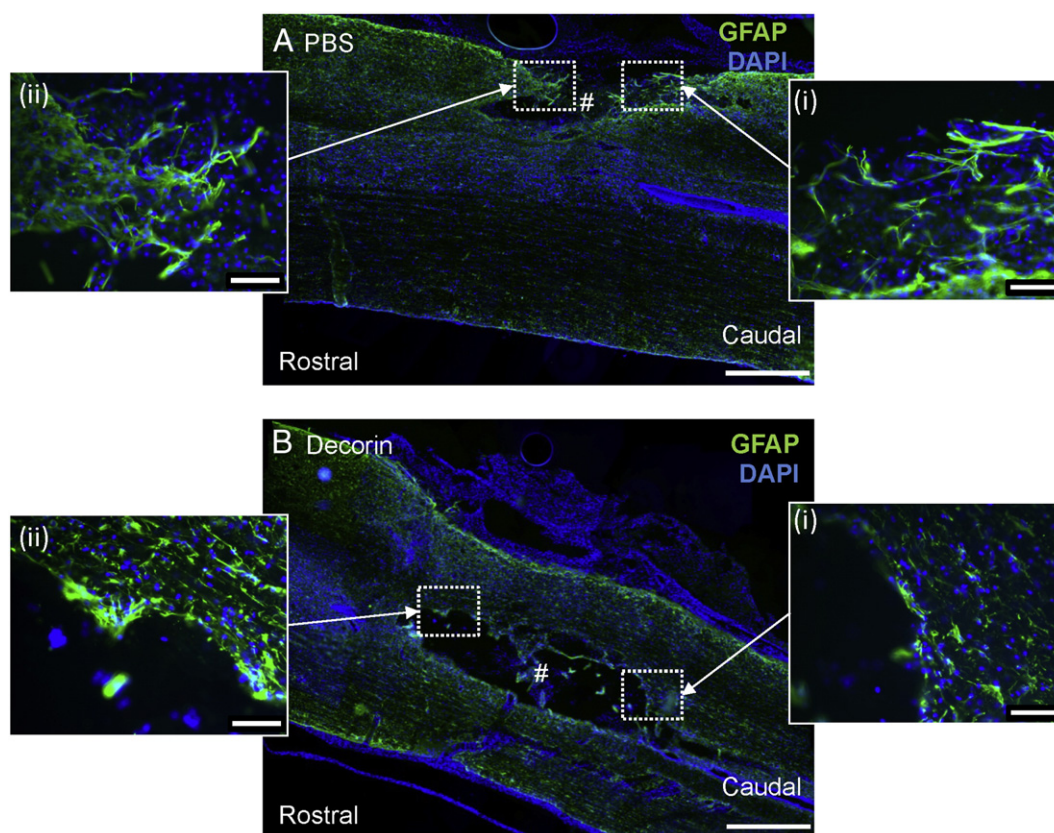


**Fig. 7.** Decorin suppresses reactive astrocytosis of chronic DFL. GFAP immunostaining of reactive astrocytes after: (A) PBS and (B) Decorin treatments. Insets i–ii show high power magnifications of the respective boxed regions (nuclei are DAPI-stained; # = lesion epicentre; scale bars = 100  $\mu$ m).

In both PBS- and Decorin-treated chronic DFL, GFAP staining was widespread throughout the lesioned cord and only present within the wound cavity in the PBS-treated group (Figs. 7A and B). Astrocyte processes were thicker and longer at the GLA in PBS-treated (Figs. 7A(i), (ii)) than in Decorin-treated wounds (Figs. 7B(i), (ii)) and, in the latter, alignment of astrocyte end-feet at the GLA basal lamina was disorganised.

These results show that Decorin attenuated the re-activation of the inflammatory response in chronic DFL and also reduced the size of the lesion by inducing dissolution of established ECM components including fibronectin and the axon growth inhibitors NG2 and Sema-3A.

#### *Effect of MMP, TIMP, tPA, PAI-1 and gelatinase activity in Decorin-treated DFL*

##### *Acute lesions*

Although levels of Pro-MMP-2 were unchanged, titres of active-MMP-2, pro- and active-MMP-9 and tPA were all significantly higher, while pro- and active-TIMP-1, pro- and active-TIMP-2 and PAI-1 levels were significantly lower in Decorin- compared to PBS-treated DFL (Figs. 8A and B; Table 2A). The ratios of active-MMP2:active-TIMP-1, active-MMP2:active-TIMP-2, active-MMP-9:active-TIMP-1, active-MMP9:active-TIMP-2 and tPA:PAI-1 were all significantly higher in Decorin- than PBS-treated DFL ( $P < 0.0001$ ; Table 3A). Zymography corroborated these results and demonstrated high levels of MMP-2 and -9 gelatinase activity in Decorin-treated DFL (Figs. 8C–G).

##### *Chronic lesions*

Pro- and active-MMP-2, pro- and active-MMP-9, and tPA were all significantly higher, while pro-TIMP-1, and pro-TIMP-2 were

significantly lower, although levels of active-TIMP-1, active-TIMP-2 and PAI-1 were not significantly different in Decorin- compared to PBS-treated DFL (Figs. 9A and B; Table 2B). The ratios of active-MMP2:active-TIMP-1, active-MMP2:active-TIMP-2, active-MMP-9:active-TIMP-1, active-MMP9:active-TIMP-2 and tPA:PAI-1 were all significantly higher in Decorin- than PBS-treated DFL ( $P < 0.05$ – $P < 0.0001$ ; Table 3B) and correlated with zymography data, which demonstrated high levels of MMP-2 and MMP-9 gelatinase activity in Decorin-treated DFL wounds (Figs. 9C–G).

Taken together, these results demonstrate that Decorin raised the levels of fibrolytic tPA and MMP activity, with a complimentary reduction in TIMP and PAI-1, more so in chronic than in acute wounds, implying that fibrolysis was responsible for dissolution of the established scar.

##### *Axonal regrowth in Decorin-treated DFL*

In both acute and chronic DFL, where a large cavity remained, GAP43<sup>+</sup> axons were absent in PBS-treated DFL (Figs. 10A–D – acute; Figs. 10E–H – chronic). However, in both acute and chronic Decorin-treated DFL, significant numbers of GAP43<sup>+</sup> axons traversed the lesion site and entered into the rostral DC neuropil (Figs. 10C and D – acute; Figs. 10G and H – chronic). GAP43<sup>+</sup> axons avoided small cavities that were present in the acute (Fig. 10 inset (i) and (ii)) and chronic (Fig. 10 inset (iii) and (iv)) Decorin-treated DFL.

## **Discussion**

The anti-fibrogenic and fibrolytic activities of Decorin were differentially dominant in reducing multiple CNS scarring parameters in acute and chronic DFL. For example, in acute DFL the anti-

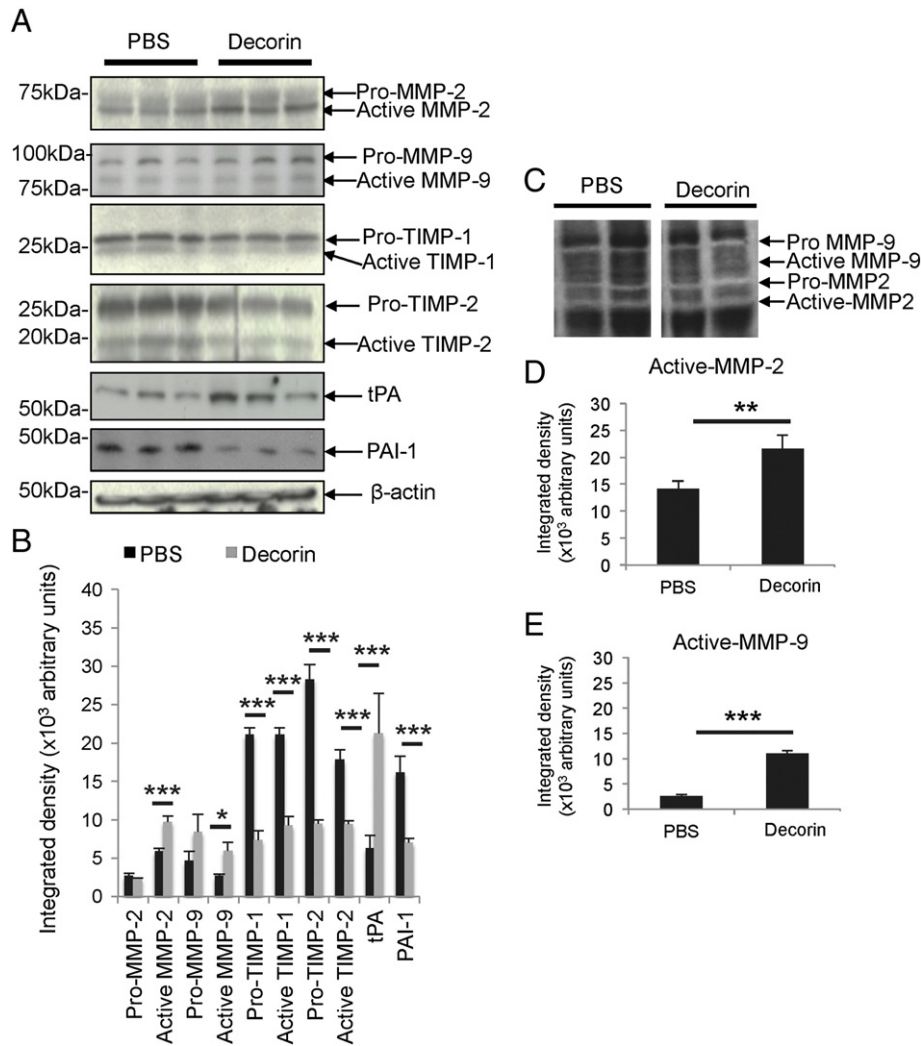


**Fig. 8.** Western blots and densitometry of MMP, TIMP, tPA, PAI-1 changes and zymography to reveal gelatinase activity after PBS and Decorin treatment in acute DFL. (A and B) Western blot and subsequent densitometry of MMP-2, MMP-9, TIMP-1, TIMP-2, tPA and PAI-1; (C) zymogram to reveal gelatinase activity (white digested bands with a dark background) along with (D) active MMP-2 and (E) active MMP-9 densitometry after PBS and Decorin treatments in acute DFL, respectively (\* $p < 0.05$ ; \*\* $p < 0.01$ ; \*\*\* $p < 0.0001$ ;  $\beta$ -actin was used as a protein loading control).

fibrogenic actions of Decorin predominated, leading to highly statistically significant reductions in scarring and wound cavitation. On the other hand in mature DFL, the Decorin-induced favourable tPA: PAI-1 and MMP:TIMP ratios potentiated tPA and MMP activity and correlated with dissolution of the fibrotic ECM elements of the established scar (Fig. 11). In both acute and chronic post-injury phases of scarring, Decorin-induced depletion of key axon growth inhibitory ligands was correlated with the growth of similar numbers of axons through both acute and chronic wounds.

**Table 2A**

Changes in MMP, TIMPs, tPA and PAI-1 in acute Decorin- compared to PBS-treated DFL.

Acute DFL				
Matrix enzyme	PBS-treated	Decorin-treated	% change	P values
Pro-MMP-2	2691 $\pm$ 346	2356 $\pm$ 70	$\downarrow$ 13%	$P > 0.05$
Active-MMP-2	5931 $\pm$ 388	9750 $\pm$ 388	$\uparrow$ 64%	$P < 0.0001$
Pro-MMP-9	4638 $\pm$ 1214	8439 $\pm$ 2317	$\uparrow$ 82%	$P < 0.0001$
Active-MMP-9	2700 $\pm$ 261	6001 $\pm$ 1088	$\uparrow$ 122%	$P < 0.0001$
Pro-TIMP-1	21096 $\pm$ 859	7397 $\pm$ 1208	$\downarrow$ 65%	$P < 0.0001$
Active-TIMP-1	21089 $\pm$ 696	9281 $\pm$ 1178	$\downarrow$ 56%	$P < 0.0001$
Pro-TIMP-2	28348 $\pm$ 1904	9527 $\pm$ 435	$\downarrow$ 66%	$P < 0.0001$
Active-TIMP-2	17831 $\pm$ 1362	9455 $\pm$ 446	$\downarrow$ 47%	$P < 0.0001$
tPA	6330 $\pm$ 1689	21268 $\pm$ 5187	$\uparrow$ 236%	$P < 0.0001$
PAI-1	16197 $\pm$ 2096	7070 $\pm$ 531	$\downarrow$ 56%	$P < 0.0001$

#### Decorin suppression of inflammation in both acute and chronic DFL

The suppression of acute phase pro-inflammatory responses and scar development in DFL by Decorin is principally explained by negative-feedback regulation of TGF- $\beta$ 1/2 after receptor binding (Hildebrand et al., 1994; Yamaguchi et al., 1990). For example, reductions in macrophage mannose and type 3 integrin  $\beta$ 2 complement receptor expression (Fitch et al., 1999) suppress ED1<sup>+</sup> macrophage invasion, lowering levels of macrophage colony-stimulating factor (MCSF) and

**Table 2B**

Changes in MMP, TIMPs, tPA and PAI-1 in chronic Decorin- compared to PBS-treated DFL.

Chronic DFL				
Matrix enzyme	PBS-treated	Decorin-treated	% change	P values
Pro-MMP-2	2040 $\pm$ 501	3541 $\pm$ 1218	$\uparrow$ 74%	$P < 0.0001$
Active-MMP-2	3464 $\pm$ 345	6613 $\pm$ 1714	$\uparrow$ 91%	$P < 0.0001$
Pro-MMP-9	24347 $\pm$ 565	31867 $\pm$ 420	$\uparrow$ 31%	$P < 0.01$
Active-MMP-9	14778 $\pm$ 180	17407 $\pm$ 471	$\uparrow$ 18%	$P < 0.05$
Pro-TIMP-1	17704 $\pm$ 180	11812 $\pm$ 715	$\downarrow$ 33%	$P < 0.01$
Active-TIMP-1	15031 $\pm$ 3961	11934 $\pm$ 1683	$\downarrow$ 21%	$P > 0.05$
Pro-TIMP-2	14101 $\pm$ 2147	7651 $\pm$ 1015	$\downarrow$ 46%	$P < 0.01$
Active-TIMP-2	7509 $\pm$ 1987	6422 $\pm$ 3019	$\downarrow$ 15%	$P > 0.05$
tPA	3786 $\pm$ 232	22024 $\pm$ 4180	$\uparrow$ 482%	$P < 0.0001$
PAI-1	11116 $\pm$ 4929	8986 $\pm$ 2997	$\downarrow$ 23%	$P > 0.05$

**Table 3A**

Changes in MMP:TIMP, tPA:PAI-1 ratios in acute Decorin- compared to PBS-treated DFL (A = Active).

Acute DFL				
Ratio	PBS-treated	Decorin-treated	% change	P values
A-MMP-2:A-TIMP-1	0.45	1.05	↑133%	P < 0.0001
A-MMP-2:A-TIMP-2	0.33	1.03	↑212%	P < 0.0001
A-MMP-9:A-TIMP-1	0.13	0.65	↑400%	P < 0.0001
A-MMP-9:A-TIMP-2	0.15	0.64	↑327%	P < 0.0001
tPA:PAI-1	0.39	3.00	↑669%	P < 0.0001

**Table 3B**

Changes in MMP:TIMP, tPA:PAI-1 ratios in chronic Decorin- compared to PBS-treated DFL (A = Active).

Chronic DFL				
Ratio	PBS-treated	Decorin-treated	% change	P values
A-MMP-2:A-TIMP-1	0.23	0.55	↑139%	P < 0.0001
A-MMP-2:A-TIMP-2	0.46	1.03	↑124%	P < 0.0001
A-MMP-9:A-TIMP-1	0.98	1.46	↑49%	P < 0.01
A-MMP-9:A-TIMP-2	1.97	2.71	↑38%	P < 0.05
tPA:PAI-1	0.34	2.45	↑621%	P < 0.0001

monocyte/macrophage anti-apoptotic factors p27 (Kip1) and p21 (Waf1) (Xaus et al., 2001) resulting in a reduction in both ECM deposition and fibrosis (Lagord et al., 2002; Logan et al., 1992). Lowered titres of MCSF may also retard the proliferation and activation of ED1<sup>+</sup> microglia (Raivich et al., 1994), which are also a local source of TGF-β1/2 (Rappolee et al., 1988; Shimojo et al., 1991). GAG side chains on the Decorin core protein have the potential to neutralise leukocyte-derived chemotactic cytokine (CCL5)-induced microglia activation (Johnson et al., 2005), down-regulating neuro-inflammation through CCL5-mediated regulation of SMAD2/3 signalling in and around the DFL (Huang et al., 2010).

Reduced numbers of ED1<sup>+</sup> macrophages in Decorin-treated chronic DFL probably reflect a similar suppression of a TGF-β1/2-induced local inflammatory response re-kindled by surgical re-exposure of the chronic wound, pial placement of the collagen matrix and injection of the peri-DFL neural parenchyma.

*Decorin suppresses DFL scar development in the acute post-injury phase of wound healing*

The anti-fibrogenic actions of Decorin in acute DFL suppress fibroblast/glia-matrix interactions through integrin-β1 and fibronectin core protein binding (Heino and Massague, 1989; Igotz et al., 1989; Schmidt et al., 1991) probably retarding meningeal fibroblast migration into the DFL and disrupting fibroblast/astrocyte interactions crucial to deposition of a laminin-rich GLA basal lamina (Bundesen et al., 2003).

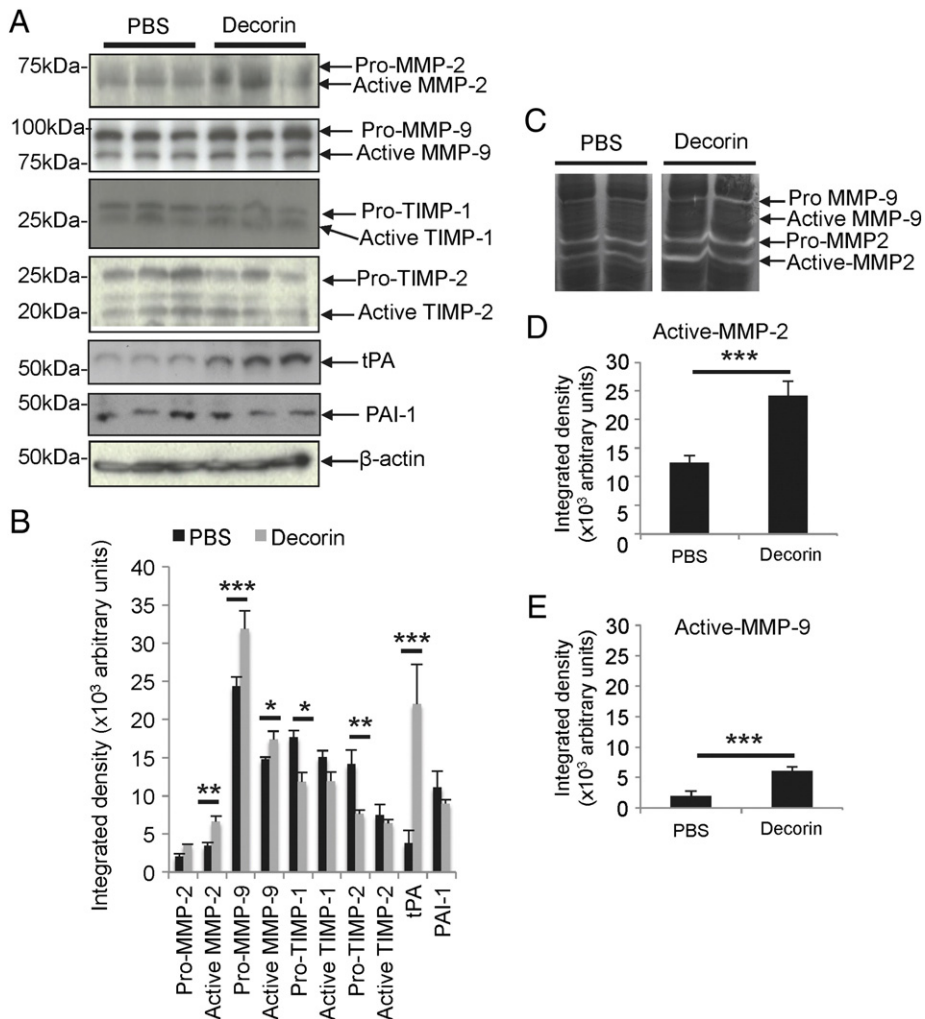


**Fig. 9.** (A and B) Western blots and densitometry of MMP-2, MMP-9, TIMP-1, TIMP-2, tPA and PAI-1; (C) zymogram to reveal gelatinase activity (white digested bands with a dark background) along with densitometry after (D) PBS and (E) Decorin treatments in acute DFL, respectively (\*p < 0.05; p < \*\*0.01; \*\*\*p < 0.0001; β-actin was used as a protein loading control).

Suppression of TGF- $\beta$ -mediated astrocytosis (Gagelin et al., 1995) is a feature of Decorin treatment in the acute and chronic periods of wound healing, characterised by thinning and poor alignment of GFAP<sup>+</sup> processes juxtaposed to the basement membrane of the GLA (Toru-Delbauffe et al., 1992), matched by a reduction in the levels of the axon growth inhibitory proteoglycan NG2 in the wound cavity. Reduced astrogliosis leads to a paucity of astrocyte-derived TGF- $\beta$ 1/2 that normally sustains the spinal cord scarring response (Hocking et al., 1998).

The morphology and reconstitution of the GLE over the DFL were not affected by Decorin probably because, in comparison with deeper disorganised injured neuropil, the peri-lesion sub-pial astrocyte/meningeal fibroblast scaffold remained mostly intact after crushing the cord, and thus adequate repair was orchestrated by interaction between a resident population of subpial astrocytes and leptomeningeal fibroblasts (Bundesen et al., 2003).

#### Decorin promotes the dissolution of established scar tissue in chronic DFL wounds

TGF- $\beta$  activity has subsided in chronic DFL and thus the observed reductions in selective scarring parameters after Decorin treatment of

chronic lesions were independent of changes in this injury responsive cytokine and are more plausibly correlated with Decorin-induced elevation in the levels of fibrolytic tPA and MMP activity, with a complementary reduction in TIMP and PAI-1. Fibrolysis reduced fibronectin in the scar, and also the axon growth inhibitory NG2 and Sema-3A components but had little effect on the glia limitans accessoria and reduced the area of the wound cavity. It is also likely that the levels of other CSPG and also ephrins are down-graded by Decorin rendering Decorin-treated wounds less inhibitory to axon growth.

#### Decorin-induced removal of axon growth inhibitory ligands from both acute and chronic DFL is correlated with axon regeneration through the wound

The blocking of scar development by Decorin reduced the acute wound cicatrix to a greater extent than that achieved in the chronic lesion by dissolution. Nonetheless, Decorin promoted the regeneration of similar small numbers of GAP43<sup>+</sup> axons through the lesions in both paradigms probably by the combined effects of clearance of axon growth inhibitory ligands from the wounds (Minor et al., 2008a), suppression of astrogliosis, protection against growth collapse by inhibition

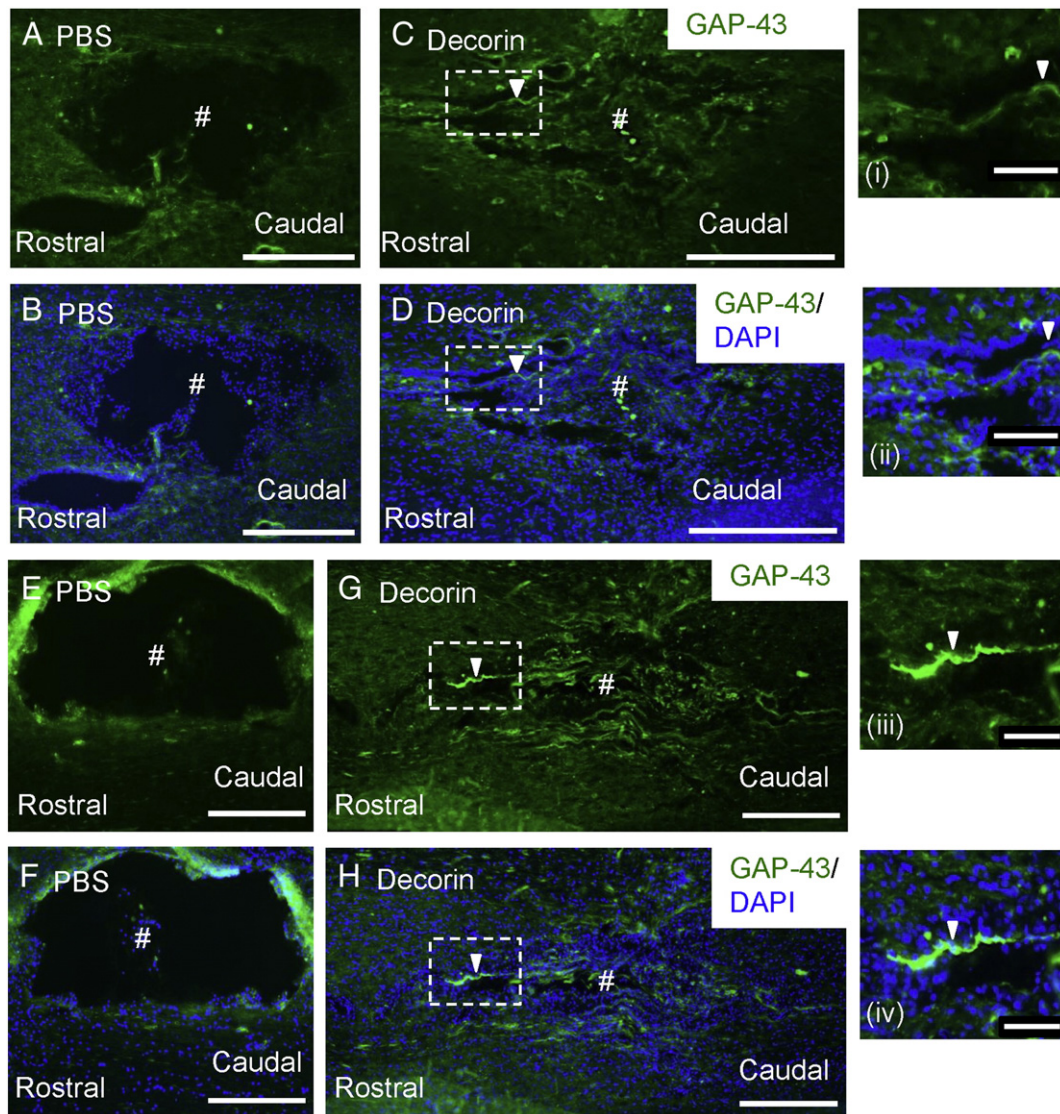


**Fig. 10.** Decorin promotes regeneration of GAP43<sup>+</sup> axons in acute and chronic DFL. In acute DFL wounds (A–D), GAP43<sup>+</sup> axons (arrowhead) were absent in PBS-treated DFL (A and B) while a significant number of axons were present in Decorin-treated DFL (C and D). Inset (i) and (ii) show high power magnifications of axons in the boxed regions of C and D, respectively. In chronic DFL wound, GAP43<sup>+</sup> axons were again absent in PBS-treated DFL (E and F) while a significant number of axons (arrowhead) were present in Decorin-treated DFL (G and H). Inset (iii) and (iv) show high power magnifications of axons in the boxed regions of (C) and (D), respectively. # = lesion epicentre; scale bars = 100  $\mu$ m.

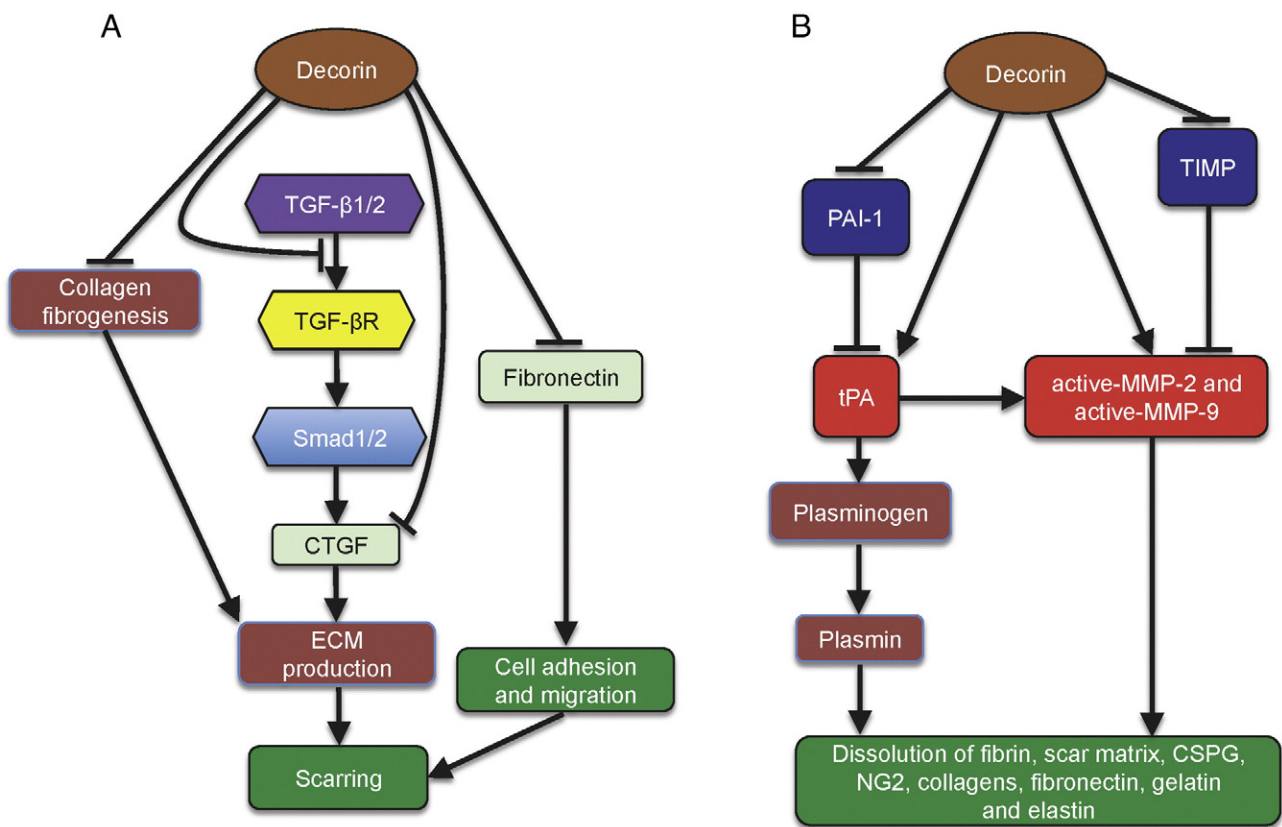


**Fig. 11.** Anti-fibrogenic (A) and fibrolytic (B) actions of Decorin. Both actions operate in acute and chronic DFL, but anti-fibrogenic actions predominate in acute and fibrolytic actions predominate in chronic DFL. (A) In acute DFL, Decorin blocks the actions of injury-induced TGF-β1/2, which normally binds to the TGF-β receptor (TGF-βR) and activates extracellular matrix (ECM) production through Smads1/2 and downstream connective tissue growth factor (CTGF). The blocking actions of Decorin on TGF-β1/2 thus attenuate acute scarring responses. Decorin also blocks collagen fibrogenesis by binding to type I collagen fibrils and binds to fibronectin to inhibit cell adhesion and migration, both of which contributes to the attenuation of scarring. (B) In chronic DFL, Decorin activates the PA system including upregulation of tPA which is tightly controlled by PAI-1. tPA principally degrades plasminogen into plasmin as a function of the fibrinolytic clotting pathway but can also cleave laminin. Enhanced levels of tPA increase the activity of MMP-2 and -9 whose activities are regulated by TIMP (TIMP-1 and -2). MMP-2 activity degrades the ECM proteins elastin, collagen, gelatin and fibronectin as well as axon growth inhibitory CSPG. MMP-9 degrades elastin, gelatin and collagens as well as the axon growth inhibitory proteoglycan NG2. Degradation of inhibitory molecules changes the environment of the spinal cord into one conducive to axon growth.

of EGFR, increased integrin expression (Matsui and Oohira, 2004) and activation of neurotrophins by elevating plasmin titres (Davies et al., 2006). ECM-degrading chondroitinases are currently undergoing extensive pre-clinical testing as a therapy for lowering the axon growth inhibitory composition of injured CNS and possibly promoting plasticity by dissolution of peri-neuronal nets (Shi et al., 2011; Wang et al., 2010). The small number of axons regenerating in this study suggests that suboptimal titres of neurotrophins are present and thus, Decorin treatment supplemented with an axogenic strategy (e.g. either mTOR activation (Liu et al., 2010) or neural stem cell implantation (Hou et al., 2013; Lu et al., 2012) might promote more effective functional recovery than either treatment alone. Decorin-induced MMP production may also support neurological recovery in damaged CNS tissues, by promoting remyelination of damaged and regenerated axons (Liu et al., 2010). Accordingly, in cases of both acute and chronic spinal cord injury, Decorin treatment has the potential to restore function by transforming the neuropil of both wound sites into a growth-permissive environment (Matsui and Oohira, 2004) and by stimulating axon growth, although the latter property may require amplification using more potent axogenic manipulations. Nonetheless, Decorin-treatment is potentially useful for the majority of chronic SCI patients who have missed the acute window for Decorin treatment since Decorin remains effective in reducing scar tissue and promoting axon regeneration in chronic lesions.

## Conclusions

Our results support the hypothesis that treatment of DFL with Decorin: (1), suppresses inflammation and scar deposition in the

acute and subacute phases of the CNS injury response by modulating TGF-β1/2-mediated fibrogenesis and by inducing MMP and tPA activity during the consolidation phase of scarring; (2), in mature scars, in which titres of TGF-β1/2 have declined, Decorin treatment causes scar dissolution by promoting tPA/MMP-mediated fibrolysis; and (3), in acute and chronic Decorin-treated wounds similar small numbers of axons traverse the lesions. Although the methods of delivery of Decorin in this experimental study are not clinically translatable, intrathecal injection of human recombinant GMP Decorin is a feasible alternative clinical delivery strategy for inhibiting the development of scarring and causing the dissolution of established scars in cord wounds and, supplemented with an axogenic therapy, has the potential to restore function in paraplegic patients.

Supplementary data to this article can be found online at <http://dx.doi.org/10.1016/j.nbd.2013.12.008>.

## Acknowledgments

This work was funded by the International Spinal Research Trust, grant no. STR103. The authors would also like to thank Dr. Andrew Thewles, Neurotrauma and Neurodegeneration, University of Birmingham, for his technical assistance with the surgery.

## References

Ahmed, Z., et al., 2005. Matrix metalloproteases: degradation of the inhibitory environment of the transected optic nerve and the scar by regenerating axons. *Mol. Cell. Neurosci.* 28, 64–78.

- Akhurst, R.J., 2006. A sweet link between TGFbeta and vascular disease? *Nat. Genet.* 38, 400–401.
- Berry, M., et al., 1983. Deposition of scar tissue in the central nervous system. *Acta Neurochir. Suppl. (Wien)* 32, 31–53.
- Berry, M., et al., 2011. Epidermal growth factor receptor antagonists and CNS axon regeneration: mechanisms and controversies. *Brain Res. Bull.* 84, 289–299.
- Boche, D., et al., 2006. TGFbeta1 regulates the inflammatory response during chronic neurodegeneration. *Neurobiol. Dis.* 22, 638–650.
- Bundesden, L.Q., et al., 2003. Ephrin-B2 and EphB2 regulation of astrocyte–meningeal fibroblast interactions in response to spinal cord lesions in adult rats. *J. Neurosci.* 23, 7789–7800.
- Butt, A.M., et al., 2002. Syntanocytes: new functions for novel NG2 expressing glia. *J. Neurocytol.* 31, 551–565.
- Davies, J.E., et al., 2004. Decorin suppresses neurocan, brevicin, phosphacan and NG2 expression and promotes axon growth across adult rat spinal cord injuries. *Eur. J. Neurosci.* 19, 1226–1242.
- Davies, J.E., et al., 2006. Decorin promotes plasminogen/plasmin expression within acute spinal cord injuries and by adult microglia in vitro. *J. Neurotrauma* 23, 397–408.
- Douglas, M.R., et al., 2009. Off-target effects of epidermal growth factor receptor antagonists mediate retinal ganglion cell disinhibited axon growth. *Brain* 132, 3102–3121.
- Fitch, M.T., et al., 1999. Cellular and molecular mechanisms of glial scarring and progressive cavitation: in vivo and in vitro analysis of inflammation-induced secondary injury after CNS trauma. *J. Neurosci.* 19, 8182–8198.
- Gagelin, C., et al., 1995. Rapid TGF beta 1 effects on actin cytoskeleton of astrocytes: comparison with other factors and implications for cell motility. *Glia* 13, 283–293.
- Hamada, Y., et al., 1996. Effects of exogenous transforming growth factor-beta 1 on spinal cord injury in rats. *Neurosci. Lett.* 203, 97–100.
- Heino, J., Massague, J., 1989. Transforming growth factor-beta switches the pattern of integrins expressed in MG-63 human osteosarcoma cells and causes a selective loss of cell adhesion to laminin. *J. Biol. Chem.* 264, 21806–21811.
- Hildebrand, A., et al., 1994. Interaction of the small interstitial proteoglycans biglycan, decorin and fibromodulin with transforming growth factor beta. *Biochem. J.* 302 (Pt 2), 527–534.
- Hocking, A.M., et al., 1998. Leucine-rich repeat glycoproteins of the extracellular matrix. *Matrix Biol.* 17, 1–19.
- Hou, S., et al., 2013. Partial restoration of cardiovascular function by embryonic neural stem cell grafts after complete spinal cord transection. *J. Neurosci.* 33, 17138–17149.
- Huang, W.C., et al., 2010. TGF-beta1 blockade of microglial chemotaxis toward Abeta aggregates involves SMAD signaling and down-regulation of CCL5. *J. Neuroinflammation* 7, 28.
- Ignotz, R.A., et al., 1989. Regulation of cell adhesion receptors by transforming growth factor-beta. Regulation of vitronectin receptor and LFA-1. *J. Biol. Chem.* 264, 389–392.
- Johnson, Z., et al., 2005. Interaction of chemokines and glycosaminoglycans: a new twist in the regulation of chemokine function with opportunities for therapeutic intervention. *Cytokine Growth Factor Rev.* 16, 625–636.
- Kawano, H., et al., 2012. Role of the lesion scar in the response to damage and repair of the central nervous system. *Cell Tissue Res.* 349, 169–180.
- Lagord, C., et al., 2002. Expression of TGFbeta2 but not TGFbeta1 correlates with the deposition of scar tissue in the lesioned spinal cord. *Mol. Cell. Neurosci.* 20, 69–92.
- Liu, K., et al., 2010. PTEN deletion enhances the regenerative ability of adult corticospinal neurons. *Nat. Neurosci.* 13, 1075–1081.
- Logan, A., et al., 1992. Enhanced expression of transforming growth factor beta 1 in the rat brain after a localized cerebral injury. *Brain Res.* 587, 216–225.
- Logan, A., et al., 1994. Effects of transforming growth factor beta 1 on scar production in the injured central nervous system of the rat. *Eur. J. Neurosci.* 6, 355–363.
- Logan, A., et al., 1999a. Decorin attenuates gliotic scar formation in the rat cerebral hemisphere. *Exp. Neurol.* 159, 504–510.
- Logan, A., et al., 1999b. Inhibition of glial scarring in the injured rat brain by a recombinant human monoclonal antibody to transforming growth factor-beta2. *Eur. J. Neurosci.* 11, 2367–2374.
- Lu, P., et al., 2012. Long-distance growth and connectivity of neural stem cells after severe spinal cord injury. *Cell* 150, 1264–1273.
- Matsui, F., Oohira, A., 2004. Proteoglycans and injury of the central nervous system. *Congenit. Anom.* 44, 181–188.
- Minor, K., et al., 2008. Decorin promotes robust axon growth on inhibitory CSPGs and myelin via a direct effect on neurons. *Neurobiol. Dis.* 32, 88–95.
- Neill, T., et al., 2012. Decorin: a guardian from the matrix. *Am. J. Pathol.* 181, 380–387.
- Pasterkamp, R.J., et al., 1999. Semaphorins and their receptors in olfactory axon guidance. *Cell. Mol. Biol. (Noisy-le-grand)* 45, 763–779.
- Pasterkamp, R.J., et al., 2001. Peripheral nerve injury fails to induce growth of lesioned ascending dorsal column axons into spinal cord scar tissue expressing the axon repellent Semaphorin3A. *Eur. J. Neurosci.* 13, 457–471.
- Raivich, G., et al., 1994. Inhibition of posttraumatic microglial proliferation in a genetic model of macrophage colony-stimulating factor deficiency in the mouse. *Eur. J. Neurosci.* 6, 1615–1618.
- Rappolee, D.A., et al., 1988. Wound macrophages express TGF-alpha and other growth factors in vivo: analysis by mRNA phenotyping. *Science* 241, 708–712.
- Reese, S.P., et al., 2013. Effects of decorin proteoglycan on fibrillogenesis, ultrastructure, and mechanics of type I collagen gels. *Matrix Biol.* 32, 414–423.
- Renckens, R., et al., 2005. The role of plasminogen activator inhibitor type 1 in the inflammatory response to local tissue injury. *J. Thromb. Haemost.* 3, 1018–1025.
- Samarakoon, R., et al., 2013. TGF-beta signaling in tissue fibrosis: redox controls, target genes and therapeutic opportunities. *Cell. Signal.* 25, 264–268.
- Sandvig, A., et al., 1994. Myelin-, reactive glia-, and scar-derived CNS axon growth inhibitors: expression, receptor signalling, and correlation with axon regeneration. *Glia* 46, 225–251.
- Schmidt, G., et al., 1991. Interaction of the small proteoglycan decorin with fibronectin. Involvement of the sequence NKISK of the core protein. *Biochem. J.* 280 (Pt 2), 411–414.
- Shi, G.D., et al., 2011. PTEN deletion prevents ischemic brain injury by activating the mTOR signaling pathway. *Biochem. Biophys. Res. Commun.* 404, 941–945.
- Shimojo, M., et al., 1991. Production of basic fibroblast growth factor in cultured rat brain microglia. *Neurosci. Lett.* 123, 229–231.
- Silver, J., Miller, J.H., 2004. Regeneration beyond the glial scar. *Nat. Rev. Neurosci.* 5, 146–156.
- Tang, X., et al., 2003. Changes in distribution, cell associations, and protein expression levels of NG2, neurocan, phosphacan, brevicin, versican V2, and tenascin-C during acute to chronic maturation of spinal cord scar tissue. *J. Neurosci. Res.* 71, 427–444.
- Toru-Delbauffe, D., et al., 1992. Effects of TGF beta 1 on the proliferation and differentiation of an immortalized astrocyte cell line: relationship with extracellular matrix. *Exp. Cell Res.* 202, 316–325.
- Vial, C., et al., 2011. Decorin interacts with connective tissue growth factor (CTGF)/CCN2 by LRR12 inhibiting its biological activity. *J. Biol. Chem.* 286, 24242–24252.
- Wang, L., et al., 2010. Deletion of Pten in pancreatic ss-cells protects against deficient ss-cell mass and function in mouse models of type 2 diabetes. *Diabetes* 59, 3117–3126.
- Winnemoller, M., et al., 1991. Influence of decorin on fibroblast adhesion to fibronectin. *Eur. J. Cell Biol.* 54, 10–17.
- Xaus, J., et al., 2001. Decorin inhibits macrophage colony-stimulating factor proliferation of macrophages and enhances cell survival through induction of p27(Kip1) and p21(Waf1). *Blood* 98, 2124–2133.
- Xu, P., et al., 2012. Post-translational regulation of TGF-beta receptor and Smad signaling. *FEBS Lett.* 586, 1871–1884.
- Yamaguchi, Y., et al., 1990. Negative regulation of transforming growth factor-beta by the proteoglycan decorin. *Nature* 346, 281–284.
- Yang, J., et al., 2011. NDRG2 ameliorates hepatic fibrosis by inhibiting the TGF-beta1/Smad pathway and altering the MMP2/TIMP2 ratio in rats. *PLoS One* 6, e27710.
- Yoshioka, N., et al., 2011. Small molecule inhibitor of type I transforming growth factor-beta receptor kinase ameliorates the inhibitory milieu in injured brain and promotes regeneration of nigrostriatal dopaminergic axons. *J. Neurosci. Res.* 89, 381–393.
- Zhang, Z., et al., 1997. Experimental analysis of progressive necrosis after spinal cord trauma in the rat: etiological role of the inflammatory response. *Exp. Neurol.* 143, 141–152.